HHS Public Access

Author manuscript

Magn Reson Med. Author manuscript; available in PMC 2023 November 01.

Published in final edited form as:

Magn Reson Med. 2022 November ; 88(5): 2259–2266. doi:10.1002/mrm.29355.

Blood-brain barrier permeability in response to caffeine challenge

Zixuan Lin[1], **Dengrong Jiang**[1], **Peiying Liu**[1], **Yulin Ge**[2], **Abhay Moghekar**[3], **Hanzhang Lu**[1,4,5]

[1]The Russell H. Morgan Department of Radiology & Radiological Science, Johns Hopkins University School of Medicine, Baltimore, Maryland, USA

[2]Department of Radiology, New York University, NY, USA

[3]Department of Neurology, Johns Hopkins University School of Medicine, Baltimore, Maryland, USA

[4]Department of Biomedical Engineering, Johns Hopkins University School of Medicine, Baltimore, Maryland, USA

[5]F. M. Kirby Research Center for Functional Brain Imaging, Kennedy Krieger Research Institute, Baltimore, Maryland, USA

Abstract

Purpose: Caffeine is known to alter brain perfusion by acting as an adenosine antagonist, but its effect on blood-brain barrier (BBB) permeability is not fully elucidated. This study aimed to dynamically monitor BBB permeability to water after a single dose of caffeine tablet using a non-contrast MRI technique.

Methods: Ten young healthy volunteers who were not regular coffee drinkers were studied. The experiment began with a pre-caffeine measurement, followed by four measurements at the post-caffeine stage. Water-extraction-with-phase-contrast-arterial-spin-tagging (WEPCAST) MRI was used to assess the time dependence of BBB permeability to water following the ingestion of 200mg caffeine. Other cerebral physiological parameters including cerebral blood flow (CBF), venous oxygenation (Y_v), and cerebral metabolic rate of oxygen ($CMRO_2$) were also examined. The relationships between cerebral physiological parameters and time were studied with mixed-effect models.

Results: It was found that after caffeine ingestion, CBF and Y_v showed a time-dependent decrease ($p<0.001$), while $CMRO_2$ did not change significantly. The fraction of arterial water crossing the BBB (E) showed a significant increase ($p<0.001$). In contrast, the permeability-surface-area product (PS), i.e. BBB permeability to water, remained constant ($p=0.94$). Additionally, it was observed that changes in physiological parameters were non-linear with regards to time and occurred at as early as 9 minutes after caffeine tablet ingestion.

Corresponding author: Hanzhang Lu, Ph.D., The Russell H. Morgan Department of Radiology and Radiological Science, Johns Hopkins University School of Medicine, 600 N. Wolfe Street, Park 322, Baltimore, MD 21287, hanzhang.lu@jhu.edu, Phone: 410-955-1431, Fax: 410-614-1977.

Conclusion: These results suggest an unchanged BBB permeability despite alterations in perfusion during a vasoconstrictive caffeine challenge.

Introduction

Caffeine, as the most widely used neurostimulant, is known to have a multifaceted effect on the human brain, especially through its role as an antagonist of adenosine (1). By binding to the adenosine receptors (mainly A_1, A_{2A} and A_{2B}) of the neurons, caffeine can block the inhibitory effect of adenosine on synaptic vesicle release and in turn increase neural activity and improve vigilance (2). On the other hand, caffeine can also constrict cerebral blood vessels by binding to the A_{2A} and A_{2B} receptors on the cerebrovascular smooth muscle, which leads to a profound change in brain hemodynamic parameters (3,4). Previous studies have reported that caffeine can cause a reduction in cerebral blood flow (CBF) and venous oxygenation (Y_v) (4–9). Through its vascular effects, caffeine has also been shown to alter temporal dynamics of BOLD response and lead to a widespread decrease in functional connectivity (10–14).

Blood-brain barrier (BBB), formed by endothelial tight junctions, astrocyte and pericytes, is a selective barrier that regulates the blood-brain exchange of substances and maintains constant microenvironment (15). All types of adenosine receptors were demonstrated to be expressed on brain capillary endothelial cells, but whether and how the adenosine receptor activation regulates BBB permeability remain unknown (16–18). As a broad-spectrum adenosine antagonist, it is useful to understand the impact of caffeine ingestion on BBB. Several prior studies have investigated the chronic effect of caffeine uptake (19,20) on BBB but not its acute effect. Furthermore, the previous studies were performed in animal models and focused on BBB permeability to large molecules such as Evan's blue dye (19,20). From a normal physiological point-of-view, it is also interesting to examine whether BBB permeability can remain stable when brain perfusion is altered by factors in daily life including breathing pattern, perspiration, or consumption of beverage containing vasoactive substances such as caffeine.

In humans, BBB permeability to gadolinium (21) can be measured with contrast agent based MRI methods, such as dynamic contrast-enhanced (DCE). Recently, there has been an increasing interest in examining the BBB permeability to water, a small molecule that may be more sensitive to subtle changes in BBB. Several non-contrast MRI techniques have been proposed by separating intravascular and extravascular spins based on their difference in spatial location, T_1, T_2 or diffusion properties (22–29). Water-extraction-with-phase-contrast-arterial-spin-tagging (WEPCAST) MRI is one of such techniques which aims to measure global water extraction fraction (E) and BBB permeability-surface-area product (PS) by selectively measuring arterial spin labeling (ASL) signals in the venous system (24,25). This method can provide an estimation of BBB permeability at around 5 min with a good test-retest reproducibility (24). Therefore, in this study, we aimed to utilize WEPCAST MRI to investigate dynamic changes in BBB permeability following a single-dose of caffeine ingestion in young healthy adults.

Methods

Participants

Ten young healthy volunteers were recruited (age 29.1±9.3 years old, 6 females and 4 males). The participants were carefully screened and did not report any health issues. None of the participants were regular coffee drinkers. The subjects reported an average of 1.1 cups of caffeine-containing drink per week. All experiments were performed on a 3T Siemens MRI system (Prisma, Siemens Healthcare, Erlangen, Germany). The experimental procedures in this study have been approved by the Institutional Review Board of the Johns Hopkins University School of Medicine. Each participant gave informed written consent before participating in the study.

Experimental Procedures

The subject was instructed to avoid any caffeine uptake for 4 hours prior to the study. The study design was: 1) baseline measurement of WEPCAST, 4 phase contrast (PC), T_2-Relaxation-Under-Spin-Tagging (TRUST) (10 min) was performed; 2) participant was taken out of the scanner, sat up on the table, ingested a 200mg caffeine tablet (equivalent to 2 cups of regular coffee) and was quickly put back into the scanner; 3) WEPCAST/PC/TRUST measurement was performed immediately after caffeine ingestion (10 min); 4) T1-weighted MPRAGE structural scan (4 min); 5) Three further repetitions of WEPCAST/PC/TRUST (10 min each). A diagram of these procedures is shown in Supporting Information Figure S1.

MRI protocols

WEPCAST MRI was performed to estimate water extraction fraction and BBB permeability index, PS. Details of WEPCAST MRI can be found in Lin et al (24,25). Briefly, a pseudo-continuous ASL module is used to label the incoming arterial blood at the cervical region. A fraction of the labeled blood is exchanged into tissue at capillary-tissue interface through BBB while the non-extracted water is drained into the venous system. By selectively measuring the ASL signal in the main draining veins of the brain, e.g. superior sagittal sinus (SSS), using a phase-contrast-encoded acquisition, a global water extraction fraction, E, can be estimated. Together with CBF (f) measurement, PS can be obtained (30):

$$PS = -\ln(1-E)\cdot f. \quad [1]$$

WEPCAST MRI was conducted in mid-sagittal plane with a labeling duration (τ) of 4000ms and a post-labeling delay (PLD) of 3000ms. Other imaging parameters were as follows: single-shot gradient echo planar imaging (EPI) readout, field of view (FOV) = 200×200mm^2, single slice, matrix = 64×64, voxel size = 3.13×3.13mm^2, slice thickness = 10mm, GRAPPA factor = 3, flip angle = 90°, repetition time (TR) = 9200ms, echo time (TE) = 9.5ms, encoding velocity (V_{enc}) = 20cm/s, number of control/label pairs = 10 and scan duration = 6min54s. An additional M_0 image with same TE and V_{enc} and a long TR = 10s was also acquired for normalization.

Global CBF was estimated with PC MRI. PC MRI was performed at four major feeding arteries (left/right internal carotid arteries and left/right vertebral arteries) to quantify global CBF. The following parameters were used (31): TR=16.0ms, TE=10.2ms, flip angle=15°, FOV=200×200×5mm^3, voxel size=0.5×0.5×5mm^3, single slice, V_{enc}=40cm/s and scan duration=13s.

We measured global venous oxygenation, Y_v, using T_2-Relaxation-Under-Spin-Tagging (TRUST) MRI (32,33). The following parameters were used: TR = 3000 ms, TE = 3.9 ms, TI=1022 ms, flip angle = 90°, FOV = 220 × 220 × 5 mm^3, voxel size = 3.4 × 3.4 × 5 mm^3, four effective TEs (eTE = 0, 40, 80, and 160 ms) with a τ_{CPMG} of 10 ms, labeling thickness = 100 mm, and scan duration = 1min27s.

A 3D T_1-weighted magnetization-prepared-rapid-acquisition-of-gradient-echo (MPRAGE) scan was acquired with the following parameters: TR=8.8ms, TE=3.8ms, shot interval=2100ms, inversion time (TI)=1100ms, flip angle=12°, FOV=208×256×160mm^3, voxel size=1×1×1mm^3, number of slices=160, sagittal orientation, and scan duration=4min3s.

Data Analysis

All MRI data were processed using in-house MATLAB (version R2016a, MathWorks, Natick, MA) scripts. Details of WEPCAST processing can be found in Lin et al. (24). Briefly, pairwise subtraction of the velocity-encoded images for control and label conditions yields arterially labeled venous signal (ΔM):

$$\Delta M = 2\alpha(1-E)M_0 e^{-\frac{\delta_v}{T_{1b}}}, \quad [2]$$

where E is water extraction fraction, α is labeling efficiency (assume to be 86%) (34), M_0 is the equilibrium magnetization and was measured from the M_0 scan mentioned above, T_{1b} is venous blood T_1 (assumed to be 1584ms) (35), δ_v is the bolus arrival time to the vein and, for the location where $\Delta M/M_0$ reaches the peak, it is $PLD + \frac{\tau}{2}$.

For PC-MRI, region of interest (ROI) was drawn manually on the complex difference images to trace the targeted arteries. Integration of the velocity, after accounting for phase foldover, within the ROI yielded flow in the units of mL/min. The summation of flux across all feeding arteries yielded total blood flow. The MPRAGE images were segmented using an automatic processing tool, MRICloud (www.MRICloud.org, Johns Hopkins University, MD) for total brain volume quantification (36). Then the global CBF was calculated as total blood flow divided by total brain volume. BBB permeability to water, i.e. PS value, was then obtained using Eq. [1].

For TRUST MRI, subtraction between control and label images yields pure labeled blood signal at SSS, which was mono-exponentially fitted as a function of eTEs to generate venous blood T_2. Blood T_2 was then converted to Y_v using an established calibration curve (37). Cerebral metabolic rate of oxygen ($CMRO_2$) was also calculated based on Fick's principle (38):

$$CMRO_2 = CBF \cdot (Y_a - Y_v) \cdot C_h, \quad [3]$$

where Y_a is arterial oxygenation (assumed to be 98%), C_h represents the oxygen carrying capability of hemoglobin and calculated as C_h=20.4*hematocrit based on previous literature. Here the hematocrit value was assumed to be 42% for male and 40% for female (39).

The time dependence of the physiological parameters (i.e. E, PS, CBF, Y_v and $CMRO_2$) was studied with a mixed-effect model. The model started with a linear term of time to examine whether the parameter changed with time. A quadratic term, time^2, was added to the model to investigate whether time-change was non-linear. Additionally, we compared each post-caffeine time point to the value during baseline with paired t-tests. A Bonferroni corrected $p<0.05$ was considered statistically significant.

Results

Figure 1 shows representative WEPCAST control, label and difference images at baseline and difference images at different time points after caffeine ingestion. As can be seen, due to the phase-contrast flow-encoded acquisition scheme, tissue signals are successfully suppressed, and vessel signals are selectively measured. At baseline, prominent signal can be seen at the SSS, representing the labeled water spins that were not extracted by the tissue and drained directly to the venous system. After caffeine uptake, WEPCAST signal decreased gradually with time, indicating that a larger fraction of water was extracted by the tissue. Peak signal along the SSS was then used to calculate water extraction fraction. Representative images of other physiological MRI sequences, PC MRI and TRUST MRI, are shown in Supporting Information Figure S2 and S3.

Time courses of the water extraction fraction, BBB permeability and other brain physiological parameters were shown in Figure 2. Table 1 summarizes results from linear mixed model analyses. When studying the linear relationship between physiological parameters and time, it was found that caffeine ingestion had a time-dependent effect Y_v, CBF, and E, but not on $CMRO_2$ or PS. Upon further adding a quadratic term, time^2, to the model, Y_v, CBF, and E, but not $CMRO_2$ or PS, showed a significant effect (Table 1), suggesting that these physiological changes are non-linear with time. At the last time point of our measurements (approximately 45 minutes after caffeine ingestion), Y_v was found to decrease by 19%, CBF decreased by 29%, E increased by 6%. Results of paired t-tests between post-caffeine and baseline (i.e. pre-caffeine) values for physiological parameters are shown in Table 2. It can be seen that changes in physiological parameters, i.e. E, CBF and Y_v, occurred as early as 9 minutes after caffeine tablet ingestion.

Discussion

Caffeine has a known effect on the neurovascular system, but its impact on the blood-brain barrier remains unclear. In this study, we dynamically measured the effect of caffeine on the BBB permeability to a small molecule, water, using a novel non-contrast technique, WEPCAST MRI. Our findings suggested that water extraction across the BBB increased after caffeine uptake. On the other hand, BBB permeability to water remained unchanged.

We also found that CBF and venous oxygenation reduced after caffeine ingestion, consistent with its known vasoconstriction effect.

BBB prevents the entry of pathogens and neurotoxins into the brain parenchyma, thus an intact BBB function is crucial for the health of the nervous system (15). Abnormalities of BBB has been implicated in a number of brain diseases, such as Alzheimer's disease (40), Parkinson's disease (41) and multiple sclerosis (42). In order to evaluate the feasibility of BBB permeability as a disease-specific marker, it is important to examine, in the healthy brain, whether BBB permeability may change with physiological maneuvers that are known to alter hemodynamics. In the present report, we used caffeine, a substance contained in many common beverages, as a physiological challenge and observed its expected effects on CBF and venous oxygenation. However, we found that BBB permeability to water remained unchanged, indicating that the permeability of a healthy BBB is relatively stable. We did observe that the amount of water molecules that were extracted across BBB, E, was increased. Although we cannot rule out other possible factors such as change in neural activity, we postulate that the increase in E was primarily attributed to a reduced CBF (see Eq. [1]), thereby longer exchange time (43,44).

One implication of our findings is that patients or participants receiving BBB MRI do not need to refrain from caffeine consumption before the exam. In many physiological MRI exams such as CBF, CBV, venous oxygenation, cerebrovascular reactivity imaging, it is often necessary to instruct the subject not to take caffeine beverages several hours before the scan in order to avoid potential biases. It appears that this is not needed for BBB MRI. Furthermore, our findings suggest that CBF can alter without corresponding changes in BBB permeability. Technically, this characteristic may be exploited for improving the reliability of BBB MRI measurement. For example, it may be possible to use hypercapnia or acetazolamide to increase CBF and enhance the BBB MRI signal, without biasing the accuracy of the PS estimation.

In view of the intricate role that BBB plays in cell signaling systems and cerebrovasculature, some animal studies have investigated the potential effect of caffeine on BBB in the context of its therapeutic effect in neurodegenerative diseases (19,20,28,45,46). For example, Chen et al. suggested that chronic ingestion of caffeine can protect against BBB damage, including mitigating the leakage to Evan's blue dye and the decrease in tight junction protein level, in animal models of Alzheimer's disease and Parkinson's disease (19,20). It has also been suggested that caffeine can help with amyloid-β clearance across the BBB (46). It was hypothesized that caffeine can control BBB permeability through blockade of adenosine receptors, inhibition of cAMP phosphodiesterase activity, and by mediating the calcium release from intracellular spaces (45). Hurtado-Alvarado et al. reported a recovery of BBB permeability to dextrans and Evan's blue after A_{2A} receptor antagonist administration in rat model of sleep deprivation (47). However, our study is different from these previous reports in several ways. First, our study mainly focused on the acute effect of caffeine challenge and all our participants were non-regular coffee drinkers, while the prior studies focused on chronic caffeine consumption. Acute ingestion of caffeine can inhibit intracellular levels of cAMP, while chronic exposure to caffeine can result in the up-regulation of adenosine receptors on endothelial cells, the activation of which can increase the cAMP level and

protect BBB against disruption (45,48,49). Second, the previous studies measured the BBB permeability to large molecules, which may be different from the permeability to water. Third, the prior reports were conducted on conditions where BBB was already leaky due to disease while our study examined normal BBB function in response to caffeine ingestion. Finally, the earlier studies were all performed in animals whereas the present report was conducted in humans.

Recently there has been a surging interest in the measurement of BBB permeability to water using MRI and some have studied the effect of caffeine challenge (25–28,50,51). For example, Wengler et al. proposed an intrinsic diffusivity based method and reported a decrease of BBB permeability to water after caffeine challenge (28). However, it should be pointed out that the method of Wengler et al. is sensitive to both tight junction integrity in endothelia and abundance of aquaporin-4 (AQP4) on the astrocyte endfeet, since the water spins have to reach the interstitial space to experience a major reduction in apparent diffusion coefficient (that is, apparent diffusion coefficient in perivascular space is quite large). The WEPCAST technique used in the present study, on the other hand, measures ASL signal in large veins, thus can differentiate perivascular signal from vessel signal. Therefore, different MRI methods on BBB permeability to water may be probing different aspects of the water exchange process. Note that there are some reports that caffeine may regulate the expression and polarity of AQP4 and may explain the observations reported in Wengler et al. (52,53).

The current study has several limitations. First, although WEPCAST MRI can estimate BBB permeability to water efficiently, it is a global method and cannot provide regional information of BBB. Previous study showed that CBF decreased at different rate in different brain regions after caffeine ingestion (5), suggesting that the caffeine effect can be region-dependent. Further technical development on measuring regional BBB permeability can provide a better understanding of the spatial dependence of the caffeine effects. Second, we did not measure the caffeine concentration in blood and different people may react differently to caffeine. However, the measurement of CBF and Y_v can be an indicator of the caffeine effect, and we did observe significant decrease for all our participants.

Conclusion

In summary, using a non-contrast technique, WEPCAST MRI, we investigated the effect of caffeine ingestion on BBB permeability to water. Our findings suggested that despite a pronounced alteration in blood flow and oxygenation, BBB water permeability remains unchanged after caffeine uptake, indicating a stable BBB function in the presence of hemodynamic changes.

Supplementary Material

Refer to Web version on PubMed Central for supplementary material.

Grant Sponsors:

This work was supported by the National Institutes of Health, R01 AG064792, RF1 AG071515, R01 NS106711, R01 NS106702, UF1NS100588, RF1 NS110041, P41 EB031771, S10 OD021648.

References

1. Ferré S Role of the Central Ascending Neurotransmitter Systems in the Psychostimulant Effects of Caffeine. Journal of Alzheimer's Disease 2010;20:S35–S49.
2. Fredholm BB, Bättig K, Holmén J, Nehlig A, Zvartau EE. Actions of caffeine in the brain with special reference to factors that contribute to its widespread use. Pharmacological Reviews 1999;51:83–133. [PubMed: 10049999]
3. Ngai AC, Coyne EF, Meno JR, West GA, Winn HR. Receptor subtypes mediating adenosine-induced dilation of cerebral arterioles. American Journal of Physiology-Heart and Circulatory Physiology 2001;280:H2329–H2335. [PubMed: 11299238]
4. Addicott MA, Yang LL, Peiffer AM, Burnett LR, Burdette JH, Chen MY, Hayasaka S, Kraft RA, Maldjian JA, Laurienti PJ. The effect of daily caffeine use on cerebral blood flow: How much caffeine can we tolerate? Human brain mapping 2009;30:3102–3114. [PubMed: 19219847]
5. Xu F, Liu P, Pekar JJ, Lu H. Does acute caffeine ingestion alter brain metabolism in young adults? NeuroImage 2015;110:39–47. [PubMed: 25644657]
6. Cameron OG, Modell JG, Hariharan M. Caffeine and human cerebral blood flow: A positron emission tomography study. Life Sciences 1990;47:1141–1146. [PubMed: 2122148]
7. Jones HE, Herning RI, Cadet JL, Griffiths RR. Caffeine withdrawal increases cerebral blood flow velocity and alters quantitative electroencephalography (EEG) activity. Psychopharmacology 2000;147:371–377. [PubMed: 10672630]
8. Buch S, Ye Y, Haacke EM. Quantifying the changes in oxygen extraction fraction and cerebral activity caused by caffeine and acetazolamide. Journal of Cerebral Blood Flow & Metabolism 2016;37:825–836. [PubMed: 27029391]
9. Zhang J, Liu T, Gupta A, Spincemaille P, Nguyen TD, Wang Y. Quantitative mapping of cerebral metabolic rate of oxygen (CMRO2) using quantitative susceptibility mapping (QSM). Magnetic Resonance in Medicine 2015;74:945–952. [PubMed: 25263499]
10. Griffeth VEM, Perthen JE, Buxton RB. Prospects for quantitative fMRI: Investigating the effects of caffeine on baseline oxygen metabolism and the response to a visual stimulus in humans. NeuroImage 2011;57:809–816. [PubMed: 21586328]
11. Laurienti PJ, Field AS, Burdette JH, Maldjian JA, Yen Y-F, Moody DM. Dietary Caffeine Consumption Modulates fMRI Measures. NeuroImage 2002;17:751–757. [PubMed: 12377150]
12. Liu TT, Behzadi Y, Restom K, Uludag K, Lu K, Buracas GT, Dubowitz DJ, Buxton RB. Caffeine alters the temporal dynamics of the visual BOLD response. NeuroImage 2004;23:1402–1413. [PubMed: 15589104]
13. Wong CW, Olafsson V, Tal O, Liu TT. Anti-correlated networks, global signal regression, and the effects of caffeine in resting-state functional MRI. NeuroImage 2012;63:356–364. [PubMed: 22743194]
14. Chen Y, Parrish TB. Caffeine's effects on cerebrovascular reactivity and coupling between cerebral blood flow and oxygen metabolism. NeuroImage 2009;44:647–652. [PubMed: 19000770]
15. Abbott NJ, Patabendige AA, Dolman DE, Yusof SR, Begley DJ. Structure and function of the blood-brain barrier. Neurobiol Dis 2010;37:13–25. [PubMed: 19664713]
16. Mills JH, Alabanza L, Weksler BB, Couraud P-O, Romero IA, Bynoe MS. Human brain endothelial cells are responsive to adenosine receptor activation. Purinergic signalling 2011;7:265–273. [PubMed: 21484089]
17. Schaddelee MP, Voorwinden HL, van Tilburg EW, Pateman TJ, Ijzerman AP, Danhof M, de Boer AG. Functional role of adenosine receptor subtypes in the regulation of blood-brain barrier permeability: possible implications for the design of synthetic adenosine derivatives. European journal of pharmaceutical sciences : official journal of the European Federation for Pharmaceutical Sciences 2003;19:13–22. [PubMed: 12729857]

18. Carman AJ, Mills JH, Krenz A, Kim DG, Bynoe MS. Adenosine receptor signaling modulates permeability of the blood-brain barrier. The Journal of neuroscience : the official journal of the Society for Neuroscience 2011;31:13272–13280. [PubMed: 21917810]
19. Chen X, Gawryluk JW, Wagener JF, Ghribi O, Geiger JD. Caffeine blocks disruption of blood brain barrier in a rabbit model of Alzheimer's disease. J Neuroinflammation 2008;5:12. [PubMed: 18387175]
20. Chen X, Lan X, Roche I, Liu R, Geiger JD. Caffeine protects against MPTP-induced blood-brain barrier dysfunction in mouse striatum. J Neurochem 2008;107:1147–1157. [PubMed: 18808450]
21. Tofts PS, Kermode AG. Measurement of the blood-brain barrier permeability and leakage space using dynamic MR imaging. 1. Fundamental concepts. Magn Reson Med 1991;17:357–367. [PubMed: 2062210]
22. Dickie BR, Parker GJM, Parkes LM. Measuring water exchange across the blood-brain barrier using MRI. Prog Nucl Magn Reson Spectrosc 2020;116:19–39. [PubMed: 32130957]
23. Gregori J, Schuff N, Kern R, Gunther M. T2-based arterial spin labeling measurements of blood to tissue water transfer in human brain. J Magn Reson Imaging 2013;37:332–342. [PubMed: 23019041]
24. Lin Z, Jiang D, Liu D, Li Y, Uh J, Hou X, Pillai JJ, Qin Q, Ge Y, Lu H. Noncontrast assessment of blood–brain barrier permeability to water: Shorter acquisition, test–retest reproducibility, and comparison with contrast-based method. Magnetic Resonance in Medicine 2021;86:143–156. [PubMed: 33559214]
25. Lin Z, Li Y, Su P, Mao D, Wei Z, Pillai JJ, Moghekar A, van Osch M, Ge Y, Lu H. Non-contrast MR imaging of blood-brain barrier permeability to water. Magn Reson Med 2018;80:1507–1520. [PubMed: 29498097]
26. Ohene Y, Harrison IF, Nahavandi P, Ismail O, Bird EV, Ottersen OP, Nagelhus EA, Thomas DL, Lythgoe MF, Wells JA. Non-invasive MRI of brain clearance pathways using multiple echo time arterial spin labelling: an aquaporin-4 study. Neuroimage 2019;188:515–523. [PubMed: 30557661]
27. Shao X, Ma SJ, Casey M, D'Orazio L, Ringman JM, Wang DJJ. Mapping water exchange across the blood-brain barrier using 3D diffusion-prepared arterial spin labeled perfusion MRI. Magn Reson Med 2019;81:3065–3079. [PubMed: 30561821]
28. Wengler K, Bangiyev L, Canli T, Duong TQ, Schweitzer ME, He X. 3D MRI of whole-brain water permeability with intrinsic diffusivity encoding of arterial labeled spin (IDEALS). Neuroimage 2019;189:401–414. [PubMed: 30682535]
29. Zhang Q, Nguyen T, Ivanidze J, Wang Y. High Resolution Water Exchange Rate Mapping using 3D Diffusion Prepared Arterial Spin Labeled Perfusion MRI. Proceedings of the International Society for Magnetic Resonance in Medicine. Virtual Conference, (Concord: International Society for Magnetic Resonance in Medicine); 2020.
30. Crone C The Permeability of Capillaries in Various Organs as Determined by Use of the 'Indicator Diffusion' Method. Acta Physiol Scand 1963;58:292–305. [PubMed: 14078649]
31. Peng S-L, Su P, Wang F-N, Cao Y, Zhang R, Lu H, Liu P. Optimization of phase-contrast MRI for the quantification of whole-brain cerebral blood flow. Journal of Magnetic Resonance Imaging 2015;42:1126–1133. [PubMed: 25676350]
32. Lu H, Ge Y. Quantitative evaluation of oxygenation in venous vessels using T2-Relaxation-Under-Spin-Tagging MRI. Magnetic Resonance in Medicine 2008;60:357–363. [PubMed: 18666116]
33. Xu F, Uh J, Liu P, Lu H. On improving the speed and reliability of T2-relaxation-under-spin-tagging (TRUST) MRI. Magn Reson Med 2012;68:198–204. [PubMed: 22127845]
34. Aslan S, Xu F, Wang PL, Uh J, Yezhuvath US, van Osch M, Lu H. Estimation of labeling efficiency in pseudocontinuous arterial spin labeling. Magn Reson Med 2010;63:765–771. [PubMed: 20187183]
35. Lu H, Clingman C, Golay X, van Zijl PC. Determining the longitudinal relaxation time (T1) of blood at 3.0 Tesla. Magn Reson Med 2004;52:679–682. [PubMed: 15334591]
36. Mori S, Wu D, Ceritoglu C, Li Y, Kolasny A, Vaillant MA, Faria AV, Oishi K, Miller MI. MRICloud: Delivering high-throughput MRI neuroinformatics as cloud-based software as a service. Computing in Science and Engineering 2016;18:21–35.

37. Lu H, Xu F, Grgac K, Liu P, Qin Q, van Zijl P. Calibration and validation of TRUST MRI for the estimation of cerebral blood oxygenation. Magn Reson Med 2012;67:42–49. [PubMed: 21590721]
38. Kety SS, Schmidt CF. THE EFFECTS OF ALTERED ARTERIAL TENSIONS OF CARBON DIOXIDE AND OXYGEN ON CEREBRAL BLOOD FLOW AND CEREBRAL OXYGEN CONSUMPTION OF NORMAL YOUNG MEN. The Journal of Clinical Investigation 1948;27:484–492. [PubMed: 16695569]
39. Peng S-L, Dumas JA, Park DC, Liu P, Filbey FM, McAdams CJ, Pinkham AE, Adinoff B, Zhang R, Lu H. Age-related increase of resting metabolic rate in the human brain. NeuroImage 2014;98:176–183. [PubMed: 24814209]
40. Erickson MA, Banks WA. Blood-brain barrier dysfunction as a cause and consequence of Alzheimer's disease. J Cereb Blood Flow Metab 2013;33:1500–1513. [PubMed: 23921899]
41. Al-Bachari S, Naish JH, Parker GJM, Emsley HCA, Parkes LM. Blood–Brain Barrier Leakage Is Increased in Parkinson's Disease. Frontiers in Physiology 2020;11.
42. Kermode AG, Thompson AJ, Tofts P, MacManus DG, Kendall BE, Kingsley DP, Moseley IF, Rudge P, McDonald WI. Breakdown of the blood-brain barrier precedes symptoms and other MRI signs of new lesions in multiple sclerosis. Pathogenetic and clinical implications. Brain : a journal of neurology 1990;113 (Pt 5):1477–1489. [PubMed: 2245307]
43. Eichling JO, Raichle ME, Grubb RL Jr., Ter-Pogossian MM. Evidence of the limitations of water as a freely diffusible tracer in brain of the rhesus monkey. Circ Res 1974;35:358–364. [PubMed: 4419687]
44. Raichle ME, Eichling JO, Straatmann MG, Welch MJ, Larson KB, Ter-Pogossian MM. Blood-brain barrier permeability of 11C-labeled alcohols and 15O-labeled water. Am J Physiol 1976;230:543–552. [PubMed: 816209]
45. Chen X, Ghribi O, Geiger JD. Caffeine Protects Against Disruptions of the Blood-Brain Barrier in Animal Models of Alzheimer's and Parkinson's Diseases. Journal of Alzheimer's Disease 2010;20:S127–S141.
46. Qosa H, Abuznait AH, Hill RA, Kaddoumi A. Enhanced Brain Amyloid-β Clearance by Rifampicin and Caffeine as a Possible Protective Mechanism Against Alzheimer's Disease. Journal of Alzheimer's Disease 2012;31:151–165.
47. Hurtado-Alvarado G, Domínguez-Salazar E, Velázquez-Moctezuma J, Gómez-González B. A2A Adenosine Receptor Antagonism Reverts the Blood-Brain Barrier Dysfunction Induced by Sleep Restriction. PLOS ONE 2016;11:e0167236. [PubMed: 27893847]
48. Fredholm BB, Bättig K, Holmén J, Nehlig A, Zvartau EE. Actions of Caffeine in the Brain with Special Reference to Factors That Contribute to Its Widespread Use. Pharmacological Reviews 1999;51:83. [PubMed: 10049999]
49. Folcik VA, Smith T, O'Bryant S et al. Treatment with BBB022A or rolipram stabilizes the blood-brain barrier in experimental autoimmune encephalomyelitis: an additional mechanism for the therapeutic effect of type IV phosphodiesterase inhibitors. Journal of neuroimmunology 1999;97:119–128. [PubMed: 10408965]
50. Dickie BR, Vandesquille M, Ulloa J, Boutin H, Parkes LM, Parker GJM. Water-exchange MRI detects subtle blood-brain barrier breakdown in Alzheimer's disease rats. Neuroimage 2019;184:349–358. [PubMed: 30219292]
51. Zhang X, Ingo C, Teeuwisse WM, Chen Z, van Osch MJP. Comparison of perfusion signal acquired by arterial spin labeling-prepared intravoxel incoherent motion (IVIM) MRI and conventional IVIM MRI to unravel the origin of the IVIM signal. Magn Reson Med 2018;79:723–729. [PubMed: 28480534]
52. Zhao Z-A, Li P, Ye S-Y et al. Perivascular AQP4 dysregulation in the hippocampal CA1 area after traumatic brain injury is alleviated by adenosine A(2A) receptor inactivation. Sci Rep 2017;7:2254–2254. [PubMed: 28533515]
53. Lee MR, Ruby CL, Hinton DJ, Choi S, Adams CA, Young Kang N, Choi DS. Striatal adenosine signaling regulates EAAT2 and astrocytic AQP4 expression and alcohol drinking in mice. Neuropsychopharmacology 2013;38:437–445. [PubMed: 23032072]

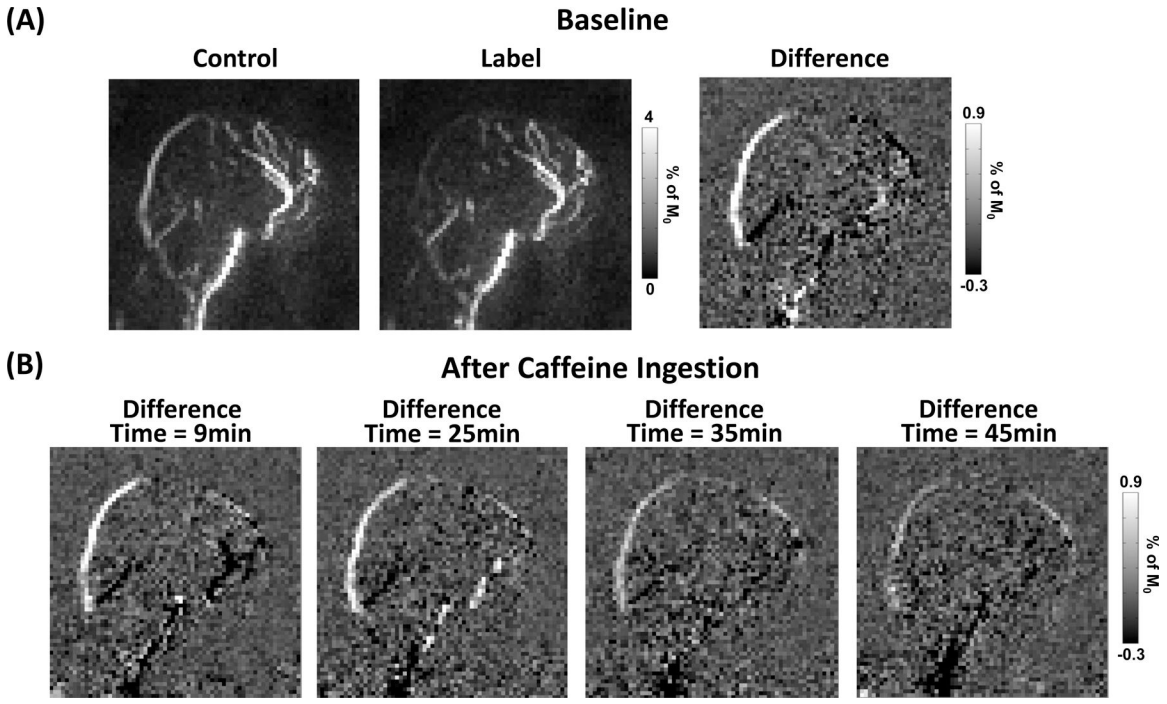

Figure 1:

Representative WEPCAST dataset in a volunteer. (A) Control, label and difference WEPCAST images at baseline. (B) WEPCAST difference images as a function of time after caffeine ingestion.

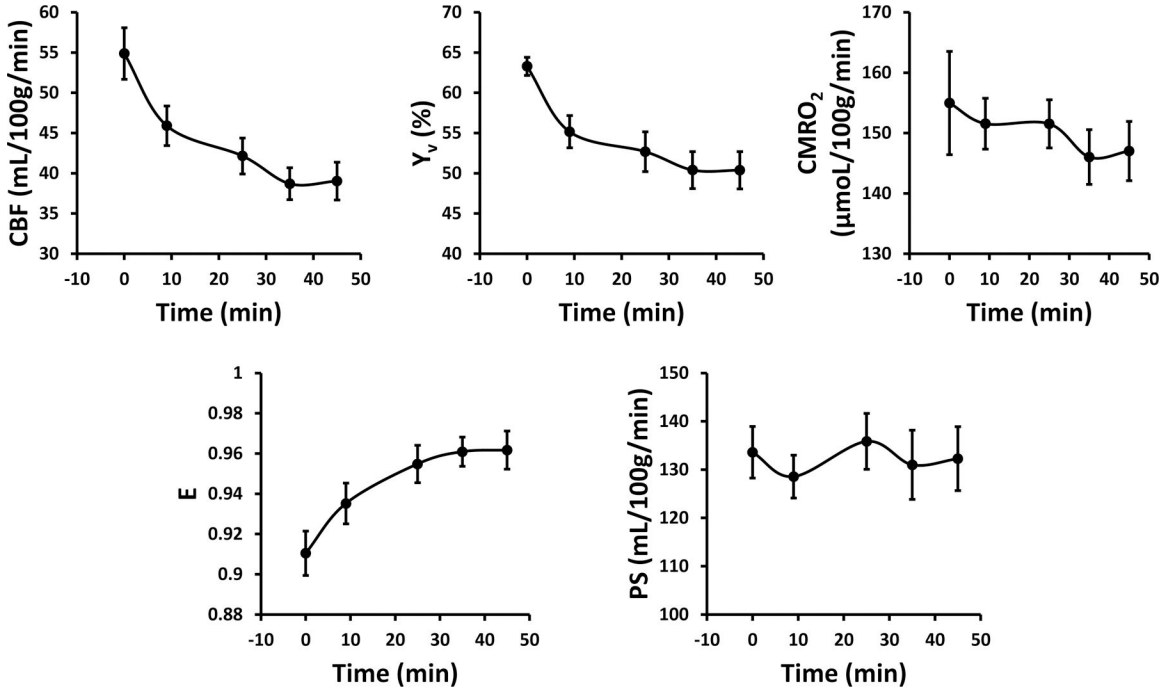

Figure 2:

Time course of cerebral blood flow (CBF), venous oxygenation (Y_v), cerebral metabolic rate of oxygen ($CMRO_2$), water extraction fraction (E), and BBB permeability-surface-area product (PS). t=0 indicates baseline measurement (i.e. before caffeine tablet ingestion). Other time points are labeled with the measurement start time (t=9min, 25min, 35min and 45min) after caffeine ingestion. Error bars denote standard errors across participants.

Table 1:

Summary of linear mixed effect model results for BBB permeability and cerebral physiology

	coefficient	std. error	p-values		coefficient	std. error	p-values
E							
Time	0.0011	0.00018	<0.0001	Time	0.0026	0.00065	0.0003
				$Time^2$	−0.000034	0.000014	0.024
PS							
Time	0.0097	0.12	0.93	Time	0.044	0.46	0.93
				$Time^2$	−0.00077	0.010	0.94
CBF							
Time	−0.33	0.047	<0.0001	Time	−0.78	0.16	<0.0001
				$Time^2$	0.010	0.0036	0.0076
Y_v							
Time	−0.26	0.030	<0.0001	Time	−0.60	0.10	<0.0001
				$Time^2$	0.0076	0.0022	0.0016
$CMRO_2$							
Time	−0.18	0.093	0.058	Time	−0.23	0.36	0.52
				$Time^2$	0.0011	0.0077	0.89

Table 2:

Summary of BBB permeability and cerebral physiology before and after caffeine uptake

	E (%)		PS		CBF		Y_v		$CMRO_2$	
	Mean±SD	**p-value***	**Mean±SD**	**p-value***	**Mean±SD**	**p-value***	**Mean±SD**	**p-value***	**Mean±SD**	**p-value***
Baseline	91.0±3.5		133.6±16.9		54.9±10.1		63.8±3.9		155.0±27.1	
Time (t) after caffeine ingestion										
t=9min	93.5±3.2	0.026	128.6±14.0	0.77	45.9±7.8	0.078	57.4±6.5	0.021	151.5±13.3	0.98
t=25min	95.5±2.9	0.0090	136.9±18.3	0.99	42.2±7.1	0.018	53.7±7.7	0.0024	151.5±12.6	0.97
t=35min	96.1±2.3	0.0039	131.0±22.7	0.99	38.7±6.3	0.0043	51.6±7.9	0.00053	146.0±14.3	0.75
t=45min	96.2±3.0	0.018	132.3±21.0	1.00	39.0±7.4	0.0035	51.6±7.6	0.00043	147.0±15.5	0.74

* p-values from paired t-test compared with baseline (Bonferroni corrected)